OPTICAL LUMINOSITIES AND MASS–TO–LIGHT RATIOS OF NEARBY GALAXY CLUSTERS

Marisa Girardi[1], Stefano Borgani[2], Giuliano Giuricin[1,3], Fabio Mardirossian[1,4], and Marino Mezzetti[1]

[1] Dipartimento di Astronomia, Università degli Studi di Trieste, Via Tiepolo 11, I-34131 Trieste, Italy
[2] INFN, Sezione di Perugia, c/o Dipartimento di Fisica dell'Università, via A. Pascoli, I-06123 Perugia, Italy;
INFN, Sezione di Trieste, c/o Dipartimento di Astronomia, Università degli Studi di Trieste, Via Tiepolo 11, I-34131 Trieste, Italy
[3]SISSA, via Beirut 4, I-34014 Trieste, Italy
[4]Osservatorio Astronomico di Trieste, Via Tiepolo 11, I-34131 Trieste, Italy
E-mail: girardi, borgani, giuricin, mardiros, mezzetti @ts.astro.it.it

ABSTRACT

We analyze a sample of 105 clusters having virial mass homogeneously estimated and for which galaxy magnitudes are available with a well defined high degree of completeness. In particular, we consider a subsample of 89 clusters with B_j band galaxy magnitudes taken from the COSMOS/UKST Southern Sky Object Catalogue.

After suitable magnitude corrections and uniform conversions to B_j band, we compute cluster luminosities L_{B_j} within several clustercentric distances, $0.5, 1.0, 1.5\ h^{-1}$ Mpc and within the virialization radius R_{vir}. In particular, we use the luminosity function and background counts estimated by Lumsden et al. (1997) on the Edinburgh/Durham Southern Galaxy Catalogue, which is the well–calibrated part of the COSMOS catalogue. We analyze the effect of several uncertainties connected to photometric data, fore/background removal, and extrapolation below the completeness limit of the photometry, in order to assess the robustness of our cluster luminosity estimates.

We draw our results on the relations between luminosity and dynamical quantities from the COSMOS sample by considering mass and luminosities determined within the virialization radius. We find a very good correlation between cluster luminosity, L_{B_j}, and galaxy velocity dispersion, σ_v, with $L_{B_j} \propto \sigma_v^{2.1–2.3}$. Our estimate of typical value for the mass-to-light ratio is $M/L_{B_j} \sim 250\ h\, M_\odot/L_\odot$. We do not find any correlation of M/L_{B_j} with cluster morphologies, i.e. Rood–Sastry and Bautz–Morgan types, and only a weak significant correlation with cluster richness.

We find that mass has a slight, but significant, tendency to increase faster than the luminosity does, $M \propto L_{B_j}^{1.2–1.3}$. We verify the robustness of this relation against a number of possible systematics. We verify that this increasing trend of M/L with cluster mass cannot be entirely due to a higher spiral fraction in poorer clusters, thus suggesting that a similar result would also be found by using R band galaxy magnitudes.

Subject headings: galaxies: clusters: general - galaxies: fundamental parameters – cosmology: observations.

1 INTRODUCTION

Since the work by Zwicky (1933), it is well known that the luminous matter associated to galaxies in clusters provides only a small part of the total cluster mass. Pioneering works typically found mass–to–optical-luminosity ratios, M/L, of several hundreds in solar units. For instance Faber & Gallagher (1979) computed M/L for seven clusters and reported a median value of $M/L_V \sim 580\ h\, M_\odot/L_\odot$, where L_V is the V band luminosity, corresponding to $M/L_B \sim 750\ h\, M_\odot/L_\odot$ when using B band luminosity (hereafter h is the Hubble constant in units of 100 km s^{-1} Mpc^{-1}). Dressler (1978b) found $M/L_R \sim$ 200–600 $h\, M_\odot/L_\odot$ for eight clusters (corresponding to about $M/L_B \sim$ 300–900 $h\, M_\odot/L_\odot$). Subsequent analyses of mass estimates based on optical and X–ray data indicated smaller values: $M/L_B = 190\ h\, M_\odot/L_\odot$ for A194 by Chapman, Geller, & Huchra (1988); $M/L_B = 200\ h\, M_\odot/L_\odot$ for Perseus cluster by Eyles et al. (1991); $M/L_V \sim$ 200–300 $h\, M_\odot/L_\odot$ for seven groups/clusters by David, Jones, & Forman (1995); $M/L_B \sim 400$ for 29 clusters of ENACS (ESO Nearby Abell Clusters Survey, Adami et al. 1998b). Small values are found also in the case of more distant clusters $M/L_R \sim 300\ h\, M_\odot/L_\odot$ (Carlberg et al. 1996 for clusters of the Canadian Network for Observational Cosmology, CNOC). However, high values of M/L have been still recently found by Mohr et al. (1996), who give $M/L_R =$ 760–1600 $h\, M_\odot/L_\odot$ for A576 from optical mass estimates.

According to the common wisdom, M/L increases from galaxy to cluster scales (e.g. Blumenthal et al. 1984), and saturates at the level of galaxy systems (see also Rubin 1993; Bahcall, Lubin, and Dorman 1995). The analysis by Rubin (1993) suggested that all systems have a constant ratio of $M/L_B \sim 200\ h\, M_\odot/L_\odot$ for scales larger than galaxies, $\sim 50 h^{-1} kpc$, so that the total mass of galaxy systems could be roughly accounted for by the total mass of their member galaxies (see also Bahcall et al. 1995).

The above results are based on M/L estimates for individual clusters or for small cluster samples. Indeed, observational difficulties prevented from building a large M/L data base, where both masses and luminosities are computed in a homogeneous way. The determination of cluster luminosities is fraught with several uncertainties, related to corrections for Galactic extinction and background galaxy contamination, calibration of the photometry, and correction of (the usual) isophotal galaxy magnitudes to total magnitudes. Further complications arise due to the need of extrapolating the sum of the measured luminosities of the cluster members to include galaxies below the completeness limit of the photometry, and to include the outer parts of the cluster beyond the region studied. These difficulties limited the number of clusters with homogeneous luminosity determinations (e.g. Oemler 1974 – 15 clusters; Dressler 1978a – 12 clusters; Adami et al. 1998a – 29 clusters; Carlberg et al. 1996 – 16 distant clusters).

Also the estimate of cluster masses is not an easy task in spite of the various methods which are applied. Cluster masses are inferred from either X–ray or optical data, under the general hypothesis of dynamical equilibrium. Estimates based on gravitational lensing do not require assumptions about the dynamical status of the cluster, but a good knowledge of the geometry of the potential well is necessary (e.g., Narayan & Bartelmann 1996). Claims for a discrepancy (by a factor of 2–3) between cluster masses obtained with different methods casted doubts about the general reliability of mass estimates (e.g., Wu & Fang 1997). However, recent analyses have shown that such discrepancies can be explained by the different way in which strong cluster substructures bias mass estimates based on different methods (Allen 1997; Girardi et al. 1997). In particular, Girardi et al. (1998b, hereafter G98) showed that, for nearby clusters without strong substructures, a good overall agreement exists between X–ray and optical mass estimates. A similar result was obtained by Lewis et al. (1999) for the distant clusters of CNOC.

The sample of 170 nearby clusters analyzed by G98 is the largest one available with homogeneous mass estimates. Therefore, this sample is suitable for M/L determinations once a proper analysis of cluster luminosities is made. To this purpose, we resort to the large homogeneous data base for B_j galaxy photometry provided by the COSMOS/UKST Southern Sky Object Catalogue (Yentis et al. 1992). We use the results from the careful work by Lumsden et al. (1997, hereafter L97) on the well-calibrated part of the COSMOS catalogue known as the Edinburgh/Durham Southern Galaxy Catalogue (EDSGC, Heydon-Dumbleton, Collins, & MacGillivray 1989). In particular, we use their best fit luminosity function and their counts of background galaxies for estimating cluster luminosities.

The paper is organized as follows. We describe the data sample and compute cluster luminosities in § 2 and § 3, respectively. The resulting luminosities and relative uncertainties are analyzed in § 4. We compute mass–to–light ratios in § 5. We devote § 6 to the analysis of the relations between luminosity and dynamical quantities. We discuss our results in § 7, while we give in § 8 a brief summary of our main results and draw our conclusions.

2 THE DATA SAMPLE

From the sample of nearby clusters ($z \leq 0.15$) analyzed by G98 we draw a subsample of 105 clusters for which galaxy magnitudes are available. In particular, we avoid the G98 clusters which show two peaks either in the velocity or in the projected galaxy distribution, as well as clusters with uncertain dynamics (cf. § 2 of G98). We also exclude A3562 which overlaps with SC1329-314 and A754, which is well–known for having a bimodal structure (e.g. Zabludoff & Zaritsky 1995). From the G98 analysis we take for each cluster: the line–of–sight velocity dispersion σ_v, the radius of virialization R_{vir}, and the virial mass M within R_{vir}. For an appropriate comparison between masses and luminosities, the latter are computed within regions centered on the same cluster centers used by G98.

2.1 The COSMOS Sample

We draw most of our results from a homogeneous sample of 89 clusters ("C–sample" hereafter) for which galaxy B_j magnitudes and positions are available from the COSMOS catalogue (Yentis et al. 1992); 20 out of these 89 clusters are in the EDSGC (Heydon-Dumbleton et al. 1989).

The EDSGC is nominally quasi–complete to $B_j = 20$. A more conservative limiting apparent magnitude was suggested by Valotto et al. (1997) who found that galaxy counts follow a uniform law for $B_j < 19.4$. Accordingly, we decide to adopt a limiting magnitude of $B_j = 19.4$ for the entire COSMOS catalog. By using data of the ESO Nearby Abell Cluster Survey (ENACS), Katgert et al. (1998) assessed that COSMOS is 91% complete and suggested that this completeness is more appropriate for areas with high surface density, rather than the nominal 95% of the catalog (Heydon-Dumbleton et al. 1989). We adopt a value of 91% for the cluster completeness in the C–sample.

For each cluster we select circular regions with a radius taken to be the largest between R_{vir} and the Abell radius (1.5 h^{-1} Mpc). For some clusters the data sample is obtained by joining data from more than one plate, since both magnitude and position inter–plate variations are small (Heydon-Dumbleton et al. 1989; Drinkwater, Barnes, and Ellison 1995).

We correct each galaxy magnitude for (1) Galactic absorption by assuming the absorption in blue band as given by de Vaucouleurs et al. (1991), and (2) K–dimming by assuming that all galaxies lie at the average cluster redshift (Colless 1989). Moreover, we apply the correction of L97 to convert COSMOS B_j magnitudes to the CCD based magnitude scale. This correction is consistent with our choice to use the luminosity function and counts by L97.

Finally, we note that COSMOS magnitudes are isopho-

tal magnitudes (the threshold is on average only 8% above the sky, cf. Heydon-Dumbleton, Collins, & MacGillivray 1988). However, Shanks, Stevenson, & Fong (1984) argue that only at faint limit (well below our limiting magnitude) the difference between COSMOS magnitudes and "total" magnitudes becomes significant.

2.2 Other Samples

In addition to the C–sample, we also analyze two cluster samples which are not homogeneus in their photometry in order to enlarge the list of available cluster luminosities as well as to perform a more accurate analysis of the errors associated to the computation of luminosities.

The second sample contains data for 39 clusters which have published galaxy positions and magnitudes down to a given completeness magnitude and are sampled at least out to 0.5 h^{-1} Mpc ("M–sample", hereafter). This sample is inhomogeneous in photometry since it contains 25, 2, and 12 clusters with photometry in blue, visual, and red bands, respectively.

A third sample ("Z–sample", hereafter) includes those 17 clusters of the M–sample, for which galaxy redshifts are also available within a certain level of completeness. We include in this sample also Ursa Major and A3558, thus ending up with 19 clusters in the Z–sample. The Ursa Major cluster data have galaxy redshifts of only cluster members up to a given completeness magnitude limit. For A3558 we use the redshift compilation by Bardelli et al. (1998, which now also include ENACS data) where magnitudes are taken from the COSMOS catalog, with a resulting completeness of 97% for $B_j < 18$ within ~ 0.75 h^{-1} Mpc.

For clusters of the M– and Z–samples we adopt the limiting magnitude and the level of completeness provided by the authors of data within the respective region of completeness. For clusters of the Z–sample we consider only galaxies identified as cluster members: for cluster data in common with G98 we use their member identification after the peak selection in velocity distribution via the adaptive kernel method and the shifting gapper (see also Fadda et al. 1996). For new cluster data we apply this same procedure for cluster member identification. The M–sample is generally superior to the Z–sample in the photometry depth (the median limiting absolute magnitude of M–clusters is $M_{B_j} = -17.6$ comparable to that of C–clusters, and only $M_{B_j} = -18.4$ for Z–clusters). The advantage of considering the Z–sample is that no fore/background subtraction is needed to estimate luminosities (§ 3).

Table 1 lists the properties of the M– and Z–samples, respectively: the source of photometric data (Col. 2); the original magnitude–band and the respective limiting apparent magnitude (Cols. 3 and 4); the completeness (Col. 5), defined as the fraction of galaxies brighter than the magnitude limit used in our analysis. For the M–samples this fraction is given by all the galaxies with measured magnitues, while for the Z–sample is given by the galaxies for which both magnitudes and redshifts are available.

TABLE 1

CLUSTER SAMPLES

Name	Refs.	Band	m_{lim}	% Compl.
M–Sample – Blue Magnitudes				
A85	1	B_j	19.75	100
A194	2	B_{Zwicky}	15.6	93
A426	3	B_{Zwicky}	15.7	100
A458	4	$B_j(APM)$	20.0	100
A539	5	B_{Zwicky}	15.7	91
A1656	6	B	20.0	100
A1656	7	B_{Zwicky}	15.7	100
A2197	8	B_{Zwicky}	15.7	100
A2554	4	$B_j(APM)$	20.2	100
A2670	9	B_j	19.0	100
A2717	4	$B_j(APM)$	18.9	100
A2721	4	$B_j(APM)$	19.7	100
A3126	4	$B_j(APM)$	18.8	100
A3128	4	$B_j(APM)$	18.5	100
A3334	4	$B_j(APM)$	20.0	100
A3360	4	$B_j(APM)$	20.0	100
A3558	10	B	20.85	100
A3574	11	B	16.0	100
A3667	12	B_j	18.0	100
A3705	4	$B_j(APM)$	20.1	100
S0753	11	B	16.6	100
S1157	4	$B_j(APM)$	19.2	100
AWM1	13	B_{Zwicky}	15.7	100
AWM7	13	B_Zwicky	15.7	100
Virgo	14	B	15.4	100
M–Sample – Visual Magnitudes				
A85	1	V	18.75	100
A1060	15	V	16.65	100
M–Sample – Red Magnitudes				
A85	1	R	18.25	100
A119	16	R	17.8	100
A539	5	R	16.83	100
A576	17	R	17.0	86
A1314	18	F	16.1	100
A2040	19	F	17.0	100
A2151	20	R	15.1	100
A2256	21	r	16.8	100
A2593	19	F	16.9	100
A2670	19	F	17.6	100
AWM4	22	R	17.5	100
MKW4	22	R	16.5	100
Z–Sample				
A0194	2	B_{Zwicky}	15.6	93
A0426	3	B_{Zwicky}	15.7	100
A0576	17	R	17.0	86
A1060	15	V	14.9	100
A1656	7	B_{Zwicky}	15.7	100
A2151	20	R	15.1	100
A2197	8	B_{Zwicky}	15.7	100
A2256	21	r	16.7	100
A2670	9	B_j	19.0	100
A3558	23,24	$B_j(COSMOS)$	18.0	88

TABLE 1

CONTINUED

Name	Refs.	Band	m_{lim}	% Compl.
A3574	11	B	15.5	100
A3667	12	B_j	17.5	91
S0753	11	B_j	15.5	100
AWM1	13	B_{Zwicky}	15.7	100
AWM4		R	15.5	100
AWM7	13	B_{Zwicky}	15.7	100
MKW4		R	15.5	94
Ursa Major	25	B	14.45	100
Virgo	14	B	15.4	89

(1) Slezak et al. 1998; (2) Chapman et al. 1988 ; (3) Kent & Sargent 1983; (4) Colless 1989; (5) Ostriker et al. 1988; (6) Godwin, Metcalfe, & Peach 1983; (7) Kent & Gunn 1982; (8) Gregory & Thompson 1984; (9) Sharples, Ellis, & Gray 1988; (10) Metcalfe et al. 1994; (11) Willmer et al. 1991; (12) Sodré et al. 1992; (13) Beers et al. 1984; (14) Binggeli, Sandage, & Tammann 1985; (15) Richter 1989; (16) Fabricant et al. 1993; (17) Mohr et al. 1996; (18) Flin et al. 1995; (19) Trevese et al. 1997; (20) Barmby & Huchra 1998; (21) Fabricant, Kent, & Kurtz 1989; (22) Malumuth & Kriss 1986; (23) Bardelli et al. 1998; (24) COSMOS catalog; (25) Tully et al. 1996

We correct each galaxy magnitude for: (1) galactic absorption by assuming the absorption in blue band as given by de Vaucouleurs et al. (1991) and transformed to visual and red bands according to Sandage (1973); (2) K–dimming by assuming that all galaxies lie at the average cluster redshift. We adopt the K–dimming corrections given by Colless (1989) for blue band, and by Sandage (1973) for visual and red bands.

Then, in order to homogeneize the photometry, we convert all magnitudes into the B_j band. In particular, since magnitudes measured by APM and COSMOS machines suffer from similar systematic effects (Metcalfe, Fong & Shanks 1995), we apply the same correction, already applied to COSMOS magnitudes, to APM magnitudes in order to convert B_j magnitudes to the CCD based magnitude scale (cf. § 2.1). We transform B band magnitudes into the B_j band by the expression $B_j = B + 0.28(B-V)$ (Blair & Gilmore 1982; see also Metcalfe et al. 1995, and Maddox, Efstathiou, & Sutherland 1990). Magnitudes in other bands are converted to the B and then to B_j band, according to the following procedure: by using eqs. (6) and (7) by Kirshner, Oemler, & Schechter (1978) for B_{Zwicky}; by using $B = V + (B-V)$ for the V band; by using $B = R + (B-V) + (V-R)$ for the R band or the F band (assuming $R = F$ as in Lugger 1989; see also Trevese, Cirimele, & Appodia 1996). In the above conversions we use the colors for the appropriate galaxy morphological type (Buta et al. 1994; Buta & Williams 1995) or, when morphology is unknown (i.e. for all C–clusters and for most of the other clusters), the typical colors of early type galaxies $(B-V) = 0.9$ and $(V-R) = 0.55$. Magnitudes in the r band by Gunn are reported to R band with $r = R + 0.35$ (Jørgensen 1994, see also Geller et al. 1997) and then to B and to B_j bands. In general, the magnitude bands are isophotal and we do not correct for this effect.

3 COMPUTING THE CLUSTER LUMINOSITIES

Observed luminosities are computed within several clustercentric regions defined by the virialization radius, R_{vir}, and by the fixed apertures 0.5, 1, 1.5 h^{-1} Mpc. We always avoid extrapolating the luminosity to include the outer parts of the clusters beyond the completeness region. Therefore, for C–clusters we can compute luminosities in all the above cluster regions, while for M– and Z–clusters we can always compute luminosities within 0.5 h^{-1} Mpc, but only in some cases within more extended regions.

Observed cluster luminosities, $L_{B_j,obs}$, are obtained by summing the individual absolute luminosities of all galaxies and assuming $B_{j,\odot} = 5.33$ (i.e. $B_\odot = 5.48$ and using the conversion to B_j by Kron 1978).

The resulting absolute luminosities and the number counts are corrected for partial sampling incompleteness of the original samples by dividing them by the nominal completeness, as provided in the literature (see Table 1). This amounts to assume that the correction for incompleteness is the same for counts and luminosities. This assumption is certainly appropriate for C–clusters, since Katgert et al. (1998) already found that the magnitude distribution of missing galaxies is essentially the same as for sampled galaxies.

Luminosities of C– and M–clusters need to be corrected for fore/background contamination. We compute the corrected luminosity, $L_{B_j,corr}$, by subtracting the average fore/background luminosity obtained from the mean field B_j counts of L97 (cf. their Figure 2) and assuming a 95% completeness for the COSMOS catalog (Heydon-Dumbleton et al. 1989). Corrected counts N_{corr} are then obtained in a similar way. The limitation of this procedure is that local fluctuations of the luminosity field are not taken into account.

As an alternative, we also consider the method recently used by Adami et al. (1998a) in the analysis of the fundamental plane of ENACS clusters. This method is based on applying suitable corrections, $L_{B_j,corr} = L_{B_j,obs} * f_L$ and $N_{corr} = N_{obs} * f_N$, under the assumption that the fraction of the luminosity, f_L, and the fraction of the number, f_N, of cluster galaxies within the selected fields in the present samples are the same as in the G98 samples. The G98 samples were collected by requiring that redshifts were available for all galaxies, thus allowing the definition of galaxy membership. We adopt $f_L = f_N$ for those G98 clusters for which magnitudes are not available.

The median fore/background correction for C– and M–clusters lies in the range $\sim$ 15–40% depending on the method and on the extension of the cluster area (in particular it is 20–30% within R_{vir}).

In order to obtain the total cluster luminosity, we need to extrapolate the above luminosities to include galaxies below the magnitude completeness limit. We adopt the usual Schechter (1976) form for the cluster luminosity function, hereafter LF, to obtain the total cluster luminos-

ity:

$$L_{B_j,tot} = L_{B_j,corr} + \Phi^* L^* \int_{L_{min}/L^*}^{L_{lim}/L^*} x^{1+\alpha} e^{-x} dx, \quad (1)$$

where $L_{B_j,corr}$ is the observed cluster luminosity corrected for incompleteness and fore/background subtraction, L_{lim} is the luminosity corresponding to the limiting magnitude, L_{min} corresponds to a cut–off for the minimum galaxy luminosity (here we adopt $L_{min} = 10^{-4} L^*$), and L^*, α, and Φ^* are the parameters of the LF. We adopt the LF parameters determined by L97, i.e. the L^* value corresponding to the absolute magnitude $M^*_{B_j} = -20.16$ and $\alpha = -1.22$. L97 derived their best fit of LF over the range -18 to -21 in M_{B_j}, for a composite sample of 22 clusters. The Φ^* parameter is determined from the observed (corrected) galaxy number counts for $-21 \leq M_{B_j} \leq -18$, $N_{corr}(-21, -18)$:

$$\Phi^* = N_{corr}(-21, -18) / \int_{L(-18)/L^*}^{L(-21)/L^*} x^{\alpha} e^{-x} dx, \quad (2)$$

where $L(-18)$ and $L(-21)$ are the luminosities corresponding to absolute magnitudes of $M_{B_j} = -18$ and $M_{B_j} = -21$, respectively. If the absolute limiting magnitude is brighter than $M_{B_j} = -18$, we take L_{lim} for the lower integration limit in eq. (2). Due to the extrapolation to faint magnitudes, the luminosity typically increases by ~ 15–20% for C– and M–clusters and more than twice for Z–clusters.

The final luminosity estimates L_{B_j} ($L_{B_j,c}$ or $L_{B_j,f}$ if the L97 counts or fractions are used for the fore/background rejection, respectively) take into account the internal galactic absorption by adopting a correction of $\Delta B_j = 0.1$ mag. Due to this correction, the luminosity increases by about 10%.

Table 2 lists the cluster luminosities: the sample to which the cluster belongs (Col. 2); the adopted cluster center (Col. 3); the number of galaxies and the cluster luminosities calculated within 0.5, 1, and 1.5 h^{-1} Mpc (Cols. 4–9); the virialization radius R_{vir} (Col. 10), the number of galaxies, $N(R_{vir})$, and the cluster luminosities, $L_{B_j}(R_{vir})$, calculated within R_{vir} (Cols. 11 and 12). We list both $L_{B_j,c}$ and $L_{B_j,f}$ within 0.5, 1 h^{-1} Mpc, and R_{vir}, while we list only $L_{B_j,c}$ within 1.5 h^{-1} Mpc (see § 4.1 below).

4 ROBUSTNESS OF LUMINOSITY ESTIMATES

Our determination of cluster luminosities is fraught with uncertainties connected to original photometric data (quality and calibration of the photometry, and completeness estimate), with magnitude corrections and conversions, as well as with uncertainties connected with the corrections applied to observed luminosities (i.e. fore/background subtraction and extrapolation to faint magnitudes). In the following we analyse possible random and systematics errors, by devoting particular care to C–clusters which will be used to obtain our main results (cf. § 6).

4.1 Estimate of fore/background Contributions

In our analysis we consider two different ways of estimating fore/background corrections in the computation of the $L_{B_j,c}$ and $L_{B_j,f}$, respectively.

As for $L_{B_j,c}$, the most direct approach would be using the L97 counts for fore/background removal. However, this method does not take into account the local field-to-field count variations, which lead to random errors. As a possible remedy, one can estimate the background for each cluster by using counts within distant external annuli. On the other hand, Rauzy, Adami, & Mazure (1998) pointed out that changes in the local field are so strong as to make this method not free of intrinsic biases (e.g., due to the presence of a nearby group along the cluster line-of-sight).

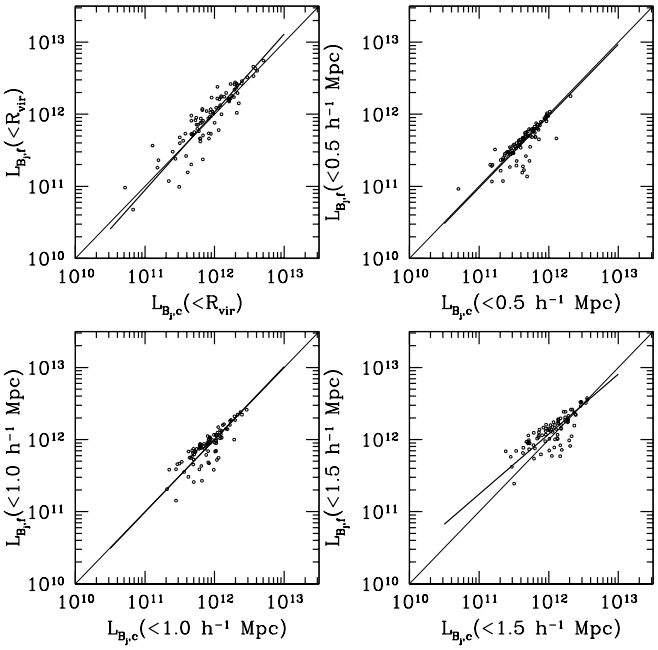

Fig. 1.— For C– clusters we show the comparison between $L_{B_j,c}$ and $L_{B_j,f}$, two alternative luminosity estimates differing for the method of fore/background correction (see text), as computed within several cluster regions. Luminosities are in units of $h^{-2}\ L_\odot$. Heavy lines represent the linear fits.

It is clear that having redshifts for all galaxies would allow an unambiguous determination of the cluster membership. By using the G98 sample of galaxy redshifts for a list of clusters, we estimate for each cluster the luminosity fraction, f_L, of galaxies which are recognized as genuine members. This fraction is then used to correct the observed luminosity. However, f_L depends on the magnitude limit and on the extension of the sampled region around the cluster. Since the G98 redshift samples are in general shallower and less spatially extended than the magnitude samples we are dealing with, this could introduce systematic errors, thus leading to an overestimate of the true

TABLE 2

LUMINOSITY ESTIMATES

Name	Sample	Center $\alpha(1950)-\delta(1950)$	$N(0.5)$	$L_{B_j}(0.5)^a$ $10^{11}h^{-2}L_\odot$	$N(1.0)$	$L_{B_j}(1.0)^a$ $10^{11}h^{-2}L_\odot$	$N(1.5)$	$L_{B_j}(1.5)^a$ $10^{11}h^{-2}L_\odot$	R_{vir} h^{-1} Mpc	$N(R_{vir})$	$L_{B_j}(R_{vir})^a$ $10^{11}h^{-2}L_\odot$
A85	C	003908.9-093501	63	4.6, 5.2	164	7.8, 8.6	287	15.1	1.94	403	20.5, 23.4
A85	M(Blue)	003908.9-093501	165	7.9, 8.5	419	17.3, 16.5	741	28.8	1.94	1036	40.1, 38.3
A85	M(Vis)	003908.9-093501	94	5.6, 6.2	242	11.5, 11.7	421	18.6	1.94	581	26.3, 28.0
A85	M(Red)	003908.9-093501	103	5.9, 6.6	265	12.3, 12.4	453	19.9	1.94	628	28.4, 29.8
A119	C	005344.7-013143	110	3.9, 4.5	263	9.8, 11.7	400	13.8	1.36	370	13.8, 17.5
A119	M(Red)	005344.7-013143	90	5.5, 6.0	211	11.9, 13.4	288	14.0	1.36	266	13.7, 17.1
A194	C	012319.6-013545	148	2.2, 2.4	427	2.8, 3.9	931	2.8	.68	218	2.5, 3.0
A194	M(Blue)	012319.6-013545	25	4.9, 4.5	47	8.6, 7.3	62	10.6	.68	33	6.3, 5.9
A194	Z	012319.6-013545	25	5.1	42	8.4	50	10.1	.68	33	6.7
A229	C	013642.7-035317	25	4.6, 5.5	50	6.9, 8.1	80	7.4	1.01	50	6.8, 8.1
A256	C	014533.0-040927	25	2.0, 2.3	75	4.9, 4.5	134	13.4	1.09	85	10.0, 7.6
A295	C	015938.9-012032	76	3.1, 2.9	227	8.8, 9.0	466	17.2	.72	137	5.9, 5.8
A420	C	030653.2-114353	29	2.0, 1.6	72	3.7, 3.5	120	4.3	.72	45	2.7, 2.4
A426	M(Blue)	031621.9+412156	40	11.9, 8.8	60	15.8, 12.7	79	17.8	2.05	105	20.3, 19.8
A426	Z	031621.9+412156	40	11.0	59	16.2	73	19.3	2.05	94	24.0
A458	C	034357.0-243001	27	5.0, 5.7	68	8.3, 10.1	118	13.7	1.47	114	12.4, 17.8
A458	M(Blue)	34357.0-243001	58	5.5, 6.5	155	11.3, 13.5	-	-	1.47	-	-
A496	C	43112.9-132322	133	2.6, 2.8	319	5.2, 6.8	610	10.6	1.37	526	7.7, 11.1
A514	C	44620.3-203847	55	3.1, 3.7	146	8.6, 10.7	249	10.9	1.76	294	11.7, 16.1
A524	C	45532.7-194823	33	2.2, 1.2	71	2.8, 1.4	117	3.2	.50	33	2.2, 1.2
A539	M(Blue)	51355.7-062436	6	7.3, 6.4	13	13.5, 11.6	22	20.0	1.26	18	16.6, 14.4
A539	M(Red)	51355.7-062436	53	3.2, 2.5	85	4.6, 3.9	-	-	1.26	-	-
A576	M(Red)	71719.1+555221	79	5.9, 5.4	180	11.7, 10.0	-	-	1.83	-	-
A576	Z	71719.1+555221	72	5.5	141	10.7	-	-	1.83	-	-
A978	C	101758.0-061546	57	2.3, 2.8	149	5.3, 6.7	219	5.2	1.07	161	5.5, 7.2
A1060	C	103410.1-2714 2	782	5.9, 5.8	2533	8.7, 10.3	5310	9.1	1.22	3678	8.8, 11.8
A1060	M(Vis)	103410.1-271402	126	4.0, 3.7	275	5.2, 5.7	-	-	1.22	-	-
A1060	Z	103410.1-271402	46	3.7	80	5.5	-	-	1.22	-	-
A1069	C	1037 6.8-081544	42	3.4, 1.9	119	7.6, 6.1	218	10.2	.72	72	6.3, 4.6
A1146	C	105850.0-222806	49	20.6, 17.8	85	29.0, 25.9	122	35.9	1.86	148	38.5, 43.2
A1314	M(Red)	113144.8 491918	55	7.2, 6.7	-	-	-	-	.55	64	7.9, 7.4
A1631	C	125020.6-150453	133	12.9, 4.6	317	19.1, 10.0	551	23.3	1.40	511	22.3, 14.2
A1644	C	125444.8-170834	142	7.7, 7.9	313	12.3, 11.8	513	17.6	1.52	524	17.9, 18.0
A1656	M(Blue)	125712.4+281323	591	10.1, 10.2	1354	16.2, 17.9	2220	22.6	1.64	-	-
A1656[b]	M(Blue)	125712.4+281323	68	16.9, 16.6	114	28.3, 28.1	151	37.3	1.64	156	38.5, 38.5
A1656	Z	125712.4+281323	68	17.0	113	28.8	150	38.6	1.64	154	39.7
A2040	M(Red)	151019.3+073633	103	7.9, 5.6	-	-	-	-	.92	-	-
A2151	M(Red)	160255.7+175332	28	7.0, 7.0	60	13.1, 13.1	79	16.1	1.50	79	19.1, 19.7
A2151	Z	160255.7+175332	27	7.1	59	13.9	72	16.5	1.50	72	16.5
A2197	M(Blue)	162806.4+405707	9	4.5, 4.7	22	11.2, 11.9	-	-	1.22	-	-
A2197	Z	162806.4+405707	9	4.7	18	9.8	-	-	1.22	-	-
A2256	M(Red)	170627.0+784227	62	14.5, 14.1	103	20.8, 21.0	138	31.1	2.70	-	-
A2256	Z	170627.0+784227	50	12.8	82	19.0	85	19.9	2.70	-	-
A2353	C	213147.4-014827	27	6.6, 7.5	44	7.9, 11.2	70	9.2	1.19	47	6.7, 11.4
A2362	C	213617.5-143242	40	1.4, 2.0	119	2.9, 4.6	199	2.4	.66	55	1.6, 2.3
A2401	C	215534.6-202015	73	4.2, 4.2	168	6.0, 7.4	285	7.2	.79	132	5.7, 6.3
A2426	C	221132.6-102555	37	5.3, 2.3	117	9.7, 3.8	209	14.6	.66	62	6.8, 2.4
A2500	C	225108.6-254700	31	2.8, 1.9	69	4.2, 3.0	125	6.1	.95	63	3.9, 2.6
A2554	C	230933.2-214708	36	7.5, 7.0	93	15.3, 13.9	159	23.2	1.68	181	24.5, 26.7
A2554	M(Blue)	230933.2-214708	74	8.6, 8.2	198	18.3, 16.9	-	-	1.68	-	-
A2569	C	231521.1-130258	38	3.5, 4.0	79	6.2, 8.7	118	5.1	.98	79	6.3, 8.7
A2593	M(Red)	232201.5+142305	62	4.7, 5.1	133	8.8, 10.4	-	-	1.40	-	-
A2644	C	233802.0-001248	29	1.5, 1.2	67	2.1, 2.1	136	3.0	.36	15	.7, .5
A2670	C	235140.5-104146	76	6.9, 6.4	159	12.6, 13.1	214	12.3	1.70	245	12.3, 17.2
A2670	M(Blue)	235140.5-104146	68	8.5, 7.8	150	16.1, 16.6	-	-	1.70	-	-
A2670	M(Red)	235140.5-104146	68	10.1, 8.9	150	19.9, 18.9	-	-	1.70	-	-

TABLE 2

CONTINUED

Name	Sample	Center $\alpha(1950)-\delta(1950)$	$N(0.5)$	$L_{B_j}(0.5)^a$ $10^{11}h^{-2}L_\odot$	$N(1.0)$	$L_{B_j}(1.0)^a$ $10^{11}h^{-2}L_\odot$	$N(1.5)$	$L_{B_j}(1.5)^a$ $10^{11}h^{-2}L_\odot$	R_{vir} $h^{-1}\ Mpc$	$N(R_{vir})$	$L_{B_j}(R_{vir})^a$ $10^{11}h^{-2}L_\odot$
A2670	Z	235140.5-104146	49	6.3	106	13.0	-	-	1.70	-	-
A2715	C	000011.6-345614	20	3.1, 2.9	50	6.4, 4.3	91	10.2	.93	46	6.2, 4.2
A2717	C	240037.3-361239	66	2.2, 2.5	156	3.1, 4.7	319	6.3	1.08	172	3.2, 4.8
A2717	M(Blue)	000037.3-361239	70	4.5, 4.3	154	8.0, 8.3	-	-	1.08	168	9.6, 9.4
A2721	C	000335.0-345944	38	6.1, 6.3	90	13.6, 16.4	138	17.5	1.61	157	19.7, 27.7
A2721	M(Blue)	000335.0-345944	69	10.2, 10.6	161	22.3, 25.0	-	-	1.61	-	-
A2734	C	000854.4-290659	51	3.2, 3.8	131	4.2, 6.8	225	5.3	1.26	184	4.6, 8.1
A2755	C	001506.4-352739	49	6.3, 5.5	105	10.1, 9.0	186	14.9	1.54	197	15.9, 15.4
A2798	C	003505.0-284835	38	7.1, 6.1	71	10.4, 11.5	117	21.3	1.42	108	20.8, 10.5
A2799	C	003457.8-392420	54	2.5, 3.0	126	4.8, 7.0	225	7.2	.84	95	3.8, 5.4
A2800	C	003535.4-252240	39	2.6, 3.0	95	4.4, 5.6	175	5.0	.81	70	3.5, 4.3
A2877	C	010734.9-4613 1	234	5.8, 6.2	530	7.0, 8.7	1015	9.9	1.77	1379	10.9, 16.5
A2911	C	012349.1-381145	40	3.9, 3.8	95	11.4, 5.6	162	19.7	1.09	106	11.5, 6.0
A3093	C	030917.6-473545	39	3.8, 3.8	80	4.6, 5.6	189	11.4	.88	71	4.6, 5.3
A3094	C	030932.3-271027	66	4.2, 4.7	164	9.2, 9.9	257	10.5	1.31	223	10.5, 12.3
A3111	C	031557.1-455754	59	4.9, 1.4	130	10.8, 5.2	228	14.7	.32	30	3.1, 1.0
A3122	C	032022.4-412948	66	2.8, 3.5	136	4.9, 6.5	216	4.8	1.55	223	4.6, 9.6
A3126	C	032716.9-555300	61	5.1, 5.0	123	8.2, 9.9	195	11.7	2.11	281	11.0, 24.0
A3126	M(Blue)	032716.9-555300	35	6.0, 5.7	74	10.7, 11.8	-	-	2.11	-	-
A3128	C	032928.3-524035	113	8.9, 8.6	285	16.6, 16.0	409	19.2	1.58	434	19.3, 21.9
A3128	M(Blue)	032928.3-524035	68	10.3, 9.8	158	20.2, 18.5	-	-	1.58	-	-
A3142	C	033455.4-395609	43	7.2, 4.5	87	10.5, 7.0	133	12.3	1.47	132	12.6, 10.0
A3151	C	033830.7-285023	61	4.2, 1.6	132	5.0, 2.6	250	11.1	.47	57	4.1, 1.6
A3158	C	034141.2-534728	137	6.3, 6.7	285	11.0, 12.4	472	17.2	1.95	669	19.4, 26.0
A3194	C	035708.7-301916	44	5.2, 6.2	109	11.3, 14.9	187	16.4	1.61	203	17.0, 26.2
A3223	C	040611.6-311045	86	4.3, 4.7	192	7.6, 8.2	300	9.1	1.29	263	9.4, 10.8
A3266	C	043007.7-614031	124	6.4, 4.9	297	12.1, 10.4	500	19.0	2.21	780	24.8, 28.9
A3334	C	051703.0-583632	35	4.2, 4.2	68	6.1, 8.3	100	6.1	1.39	96	6.7, 11.9
A3334	M(Blue)	051703.0-583632	69	5.5, 5.5	148	8.6, 11.1	-	-	1.39	-	-
A3354	C	053245.2-284245	52	3.0, 2.9	184	10.2, 6.8	331	13.3	.72	102	8.2, 5.4
A3360	C	053836.6-432531	31	4.5, 4.6	77	6.2, 8.6	115	8.4	1.67	140	9.1, 17.1
A3360	M(Blue)	053836.6-432531	67	5.0, 5.0	157	9.8, 11.9	-	-	1.67	-	-
A3376	C	060037.8-395622	73	2.7, 3.0	203	5.3, 6.8	309	5.1	1.38	288	5.4, 8.9
A3381	C	060807.6-333244	110	4.4, 1.7	273	6.6, 2.7	537	15.4	.59	126	4.6, 2.0
A3391	C	062514.2-533953	72	4.9, 4.9	189	10.7, 10.2	339	18.1	1.33	278	16.3, 16.4
A3395	C	062634.7-542433	113	5.7, 4.8	261	10.6, 8.9	425	15.1	1.70	496	16.0, 15.9
A3532	C	125432.5-300451	91	6.4, 4.8	252	12.7, 10.6	467	18.8	1.48	463	18.9, 17.3
A3556	C	132130.3-312641	93	4.7, 4.9	251	10.5, 9.6	547	24.4	1.28	409	16.2, 15.0
A3558	C	132507.1-311347	171	8.7, 8.8	467	23.5, 24.0	805	35.6	1.95	1151	50.3, 55.5
A3558	M(Blue)	132507.1-311347	369	8.3, 8.8	-	-	-	-	1.95	-	-
A3558	Z	132507.1-311347	53	9.7	-	-	-	-	1.95	-	-
A3559	C	132723.9-291830	91	6.0, 6.3	248	10.7, 11.7	489	20.4	.91	215	9.5, 10.3
A3571	C	134428.3-323710	255	10.4, 10.9	644	19.3, 21.1	1087	28.5	2.09	1746	36.0, 45.7
A3574	C	134558.3-301238	433	6.1, 5.8	1337	8.5, 9.3	2595	11.3	.98	1303	8.6, 9.2
A3574	M(Blue)	134558.3-301238	38	4.2, 3.9	-	-	-	-	.98	-	-
A3574	Z	134558.3-301238	21	3.7	-	-	-	-	.98	-	-
A3651	C	194826.9-551552	111	9.1, 9.4	264	16.6, 18.1	428	24.4	1.25	348	21.3, 19.7
A3667	C	200825.8-565733	131	9.8, 9.5	371	21.4, 22.2	646	29.6	1.94	882	40.8, 40.1
A3667	M(Blue)	200825.8-565733	43	6.3, 6.0	110	15.1, 15.4	158	19.2	1.94	-	-
A3667	Z	200825.8-565733	19	5.6	53	14.7	73	19.4	1.94	-	-
A3693	C	203110.2-344325	42	4.3, 1.9	90	8.1, 4.8	166	13.4	.96	89	8.3, 4.6
A3695	C	203133.1-355824	60	9.5, 10.3	136	17.2, 18.7	210	20.8	1.56	214	20.6, 26.6
A3705	C	203900.1-352256	73	9.1, 8.7	174	19.7, 18.7	288	28.7	1.75	327	29.6, 32.4
A3705	M(Blue)	203900.1-352256	70	7.8, 7.5	169	15.0, 15.1	-	-	1.75	-	-
A3733	C	205836.0-281416	83	2.9, 3.3	240	5.5, 7.4	414	5.2	1.22	301	5.3, 8.3
A3744	C	210427.9-253800	107	3.7, 4.3	330	6.5, 7.7	597	8.0	1.02	340	6.6, 7.8

TABLE 2

CONTINUED

Name	Sample	Center $\alpha(1950)-\delta(1950)$	$N(0.5)$	$L_{B_j}(0.5)^a$ $10^{11}h^{-2}L_\odot$	$N(1.0)$	$L_{B_j}(1.0)^a$ $10^{11}h^{-2}L_\odot$	$N(1.5)$	$L_{B_j}(1.5)^a$ $10^{11}h^{-2}L_\odot$	R_{vir} h^{-1} Mpc	$N(R_{vir})$	$L_{B_j}(R_{vir})^a$ $10^{11}h^{-2}L_\odot$
A3809	C	214405.9-440914	63	3.3, 3.6	172	6.1, 7.7	293	7.1	.96	162	5.8, 7.1
A3822	C	215043.8-580510	120	9.3, 8.0	329	24.8, 22.2	506	34.2	1.62	545	36.3, 33.8
A3825	C	215444.4-603244	80	5.5, 5.0	186	11.9, 11.3	328	18.6	1.40	298	17.0, 16.6
A3879	C	222414.3-6911 3	49	3.8, 4.1	97	4.7, 5.8	170	5.2	.80	81	4.9, 5.2
A3880	C	222502.0-304936	64	3.0, 3.2	151	6.2, 7.9	299	13.7	1.65	365	14.7, 19.7
A3921	C	224645.3-643942	47	6.9, 7.2	118	12.0, 13.5	186	14.8	.98	117	12.1, 13.4
A4008	C	232739.1-393210	59	3.4, 3.4	156	5.1, 6.2	275	6.8	.85	126	4.7, 5.3
A4010	C	232851.7-364643	37	4.7, 5.6	82	7.9, 9.0	139	13.7	1.25	102	8.7, 10.6
A4053	C	235207.7-275757	43	3.5, 2.2	109	6.0, 3.9	178	7.7	1.23	136	6.2, 4.6
A4067	C	235621.3-605412	33	3.6, 3.7	84	8.1, 8.7	134	9.0	1.00	84	8.1, 8.7
S84	C	004659.4-294712	35	5.4, 3.5	71	8.1, 6.9	105	8.9	.66	50	6.8, 5.1
S373	C	033408.4-352339	2631	1.7, 3.2	10793	*, 7.8	22620	*	.62	4150	1.3, 3.7
S463	C	042802.5-535644	151	9.4, 9.8	327	14.6, 14.2	566	18.8	1.22	416	15.8, 16.2
S721	C	130316.8-372100	123	4.0, 3.4	298	7.3, 7.5	524	12.7	1.38	463	11.4, 12.2
S753	C	140019.9-334851	423	2.9, 2.8	1451	5.0, 5.3	3299	6.1	1.07	1653	5.1, 5.7
S753	M(Blue)	140019.9-334851	33	2.6, 2.3	-	-	-	-	1.07	-	-
S753	Z	140019.9-334851	17	2.6	-	-	-	-	1.07	-	-
S805	C	184802.7-631810	402	1.6, 2.0	1843	5.0, 7.5	4149	10.0	1.08	2133	6.3, 7.6
S987	C	215907.1-223859	43	5.5, 6.1	121	13.1, 15.9	232	21.8	1.35	206	21.4, 25.4
S1157	C	234903.9-344355	43	4.7, 2.6	152	8.3, 4.7	274	12.0	1.16	191	8.9, 5.4
S1157	M(Blue)	234903.9-344355	46	5.1, 2.8	151	11.1, 5.8	-	-	1.16	-	-
AWM1	M(Blue)	091411.5 201434	11	5.1, 5.0	19	8.3, 8.7	-	-	.88	19	8.4, 8.7
AWM1	Z	091411.5 201434	11	5.1	19	8.8	-	-	.88	19	8.8
AWM4	M(Red)	160247.7+240437	38	1.5, .9	-	-	-	-	.24	20	1.3, .6
AWM4	Z	160247.7+240437	7	1.4	-	-	-	-	.24	-	-
AWM7	M(Blue)	025122.7+412330	14	3.0, 2.6	-	-	-	-	1.73	-	-
AWM7	Z	025122.7+412330	14	3.2	-	-	-	-	1.73	-	-
DC0003-50	C	000332.2-505524	85	2.3, 2.7	254	3.4, 4.9	477	4.3	.70	146	3.2, 4.0
Eridanus	C	033759.4-184707	1386	.5, .9	5270	*, 15.0	11730	*	.53	1536	.5, 1.0
MKW1	C	095812.1-024317	208	1.5, 1.9	676	2.2, 3.8	1495	3.4	.45	185	1.5, 1.8
MKW4	M(Red)	120146.5+020748	47	2.4, 2.4	-	-	-	-	1.05	-	-
MKW4	Z	120146.5+020748	24	2.8	-	-	-	-	1.05	-	-
Ursa Major	Z	115454.1+511207	23	.5	-	-	-	-	.26	8	.2
Virgo	M(Blue)	122332.4+130259	145	1.8, 2.8	-	-	-	-	1.26	-	-
Virgo	Z	122332.4+130259	101	3.5	-	-	-	-	1.26	-	-

[a] For C– and M–clusters we report both $L_{B_j,c}$ and $L_{B_j,f}$ within 0.5 and 1.0 h^{-1} Mpc , and R_{vir}; we report only $L_{B_j,c}$ within 1.5. The asterisk, $*$, denotes luminosity estimates which result negative values; this happens for two poor clusters (S753 and Eridanus) whose local galaxy field is much poorer than the mean field.

[b] The sample of A1656 in B_{Zwicky}–magnitude band (cf. Table 1).

$L_{B_j,f}$. In addition to this systematic uncertainty, there is also a random uncertainty due to the fact that the G98 sample has neither a homogeneous magnitude limit nor a uniform spatial extension around each cluster.

In order to estimate by how much such uncertainties affect our estimates of cluster luminosities, we compare in Figure 1 $L_{B_j,c}$ and L_{B_jf} for C–clusters within different radii. It is apparent that these two alternative estimates are in overall agreement, although within some scatter. While the scatter provides an estimate of the random errors, the agreement indicates that any sistematic bias should not seriously pollute our analysis. For instance, for C–clusters we find a scatter of $\sim 30\%$ and $L_{B_j,c}/L_{B_j,f} = 0.88$ for luminosities estimated within R_{vir}. Somewhat different results hold for luminosities within 1.5 h^{-1} Mpc (cf. lower–right panel in Fig. 1). In this case, the discrepancy is due to the fact that redshift data generally sample clusters only out to their typical size. This turns into high, unreliable $L_{B_j,f}$ determinations when poor clusters are examined within the large region encompassed by the $1.5h^{-1}$ Mpc radius. For this reason we do not report in Table 2 $L_{B_j,f}$ luminosities computed within this radius.

Another way of assessing the impact of fore/background corrections is based on comparing the luminosities of the Z–clusters, which are free from these corrections (cf. §2.2), with those of the corresponding M–clusters (or C–cluster for A3558), which have the same original photometry. For this comparison we use luminosities within 0.5 h^{-1} Mpc, so as to maximize the number of clusters (18) which belong to both samples. Figure 2 shows that there is no appreciable

systematic effect and that the scatter is about 10%. Allowing for larger and deeper data samples, it is reasonable to expect that the contribution of fore/background corrections to random errors increases to $\sim 20\%$, thus comparable to the above estimate of the scatter (cf. Fig. 1).

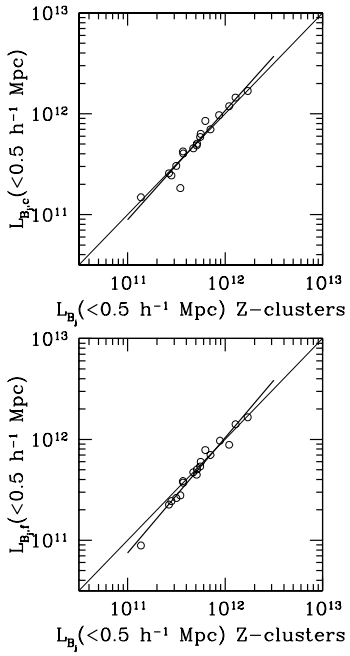

Fig. 2.— The comparison between luminosities computed for Z–clusters (which do not need fore/background correction) and the corresponding clusters in C– and M– samples, which have the same original photometry and which require fore/background correction. We consider both $L_{B_j,c}$ (top–panel) and $L_{B_j,f}$ (bottom–panel). Luminosities are in units of $h^{-2}\ L_\odot$. Heavy lines represent the linear fits.

As a further test of the robustness of our results, we consider those 51 C–clusters whose corresponding redshift samples are based on ENACS data and compare our derived f_L with those by the original ENACS analysis of Adami et al. (1998a). They analyzed well sampled ENACS clusters and found that their luminosity fractions, $f_L(ENACS)$, are not significantly biased with respect to those appropriate for COSMOS data. They found $f_L(ENACS) = 0.83$ within a typical area of 1 h^{-1} Mpc^2, thus quite similar to our median f_L of 0.88 within 0.5 h^{-1} Mpc.

As for the estimates of $L_{B_j,c}$, in order to ulteriorly check the effect of systematic uncertainties from fore/background corrections, we resort to the background galaxy counts by L97. These counts have been estimated from the large area ($\sim$ 0.5 sr) of the EDSGC, which is the well–calibrated part of the COSMOS catalogue. L97 found a general consistency with the previous results by Maddox et al. (1990b), which is the only other analysis based on a significantly large area (i.e., the APM sample), where automated procedures to estimate magnitudes have been applied. A 20% larger estimate is reported by Colless (1989) who, however, used data from smaller areas. Even using this larger background estimate, we find that $L_{B_j,c}$ only decreases by $\lesssim 10\%$.

4.2 The Extrapolation to Faint Galaxies

The precise amount of the luminosity correction due to the extrapolation to faint galaxies depends on the assumed cluster galaxy LF. Here we assume the usual Schechter form (1976) with parameters estimated by L97. As for the LF parameters, there is a general good agreement among several determination of M^*, while significantly different determinations of the parameter α have been found by other authors (cf. Rauzy et al. 1998). Such determinations typically vary in the range $-1.5, -1$ (see also Marinoni et al. 1999 for a discussion on this point). We find for C–clusters that the medians of the luminosity variations are +18% (−6%) when considering $\alpha = -1.5$ ($\alpha = -1.0$) instead of $\alpha = -1.22$, as adopted by L97.

Furthermore, we also consider the possibility of a steepening of the LF at its faint magnitudes (e.g. Biviano et al. 1995; De Propris & Pritchet 1998; Trentham 1998) with respect to a Schechter LF. In particular, the comprehensive work by Trentham (1998) shows that the local slope of the LF steepens from $\alpha \sim -1.4$ at $M_B \sim -16$ and -15 mag to $\alpha \sim -1.8$ at $M_B \sim -11$ mag. Following Zucca et al. (1997), we consider here a simplified model based on a Schechter function and a power law for the high– and low–luminosity part of the LF and use their same parameters, $\beta = -1.6$ for the exponent of the power law and $M_{B_j} = -17$ for the luminosity which separates the two LF regimes. As a result, we find that luminosities increases by less than 10%.

Our LF extrapolation to faint magnitudes implicitely assumes that there is no spatial variations of the LF within each cluster and among different clusters. These assumptions are supported by several evidences (e.g., Lugger 1986; Colless 1989; Metcalfe, Godwin, & Peach 1994; Valotto et al. 1997; Trentham 1998; Rauzy et al. 1998; see, however, Driver, Couch & Phillips 1998). In the present analysis we assume that possible differences lead to random errors which are comparable to the above $\sim$ 10% systematics. This point will be further discussed in § 6.3 below, when we will discuss possible systematics affecting the M–L_{B_j} relation.

4.3 Comparison between C– vs. M–Luminosities

We estimate the errors connected with the original photometric samples (magnitudes and nominal completeness) and with our corrections/conversions of magnitudes by comparing luminosities computed for C–clusters to those computed for the same clusters in the M–sample. Figure 3 shows the result of the comparison for the 22 clusters in common. There is no evidence of a significant systematic effect, although within a rather large scatter ($\sim$ 20%).

4.4 Error Estimates

From the above analysis we estimate that both random and systematic errors in the cluster luminosities are $\sim 20-30\%$. Finally, we stress that our luminosities have been computed by using the cluster centers reported in Table 2. After recomputing luminosities for 34 C–clusters with X–ray determined centers (Ebeling et al. 1997), which differ by $\sim 0.1\ h^{-1}$ Mpc from the optical centers we adopt in this work, we find a typical difference of $\sim 5\%$ for luminosities within R_{vir} and of $\sim 10\%$ for luminosities within $0.5\ h^{-1}$ Mpc. Since the centers we use for luminosities are the same used by G98 for mass determinations, this kind of error is not taken into account in our following analysis.

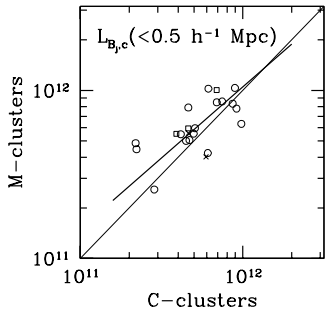

Fig. 3.— The comparison between $L_{B_j,c}$ luminosities computed for C–clusters and the corresponding clusters in M– sample, which differ for the original photometry. Circles, crosses, and squares denote original blue, visual, and red magnitudes, respectively. Luminosities are units of $h^{-2}\ L_\odot$. The heavy line represents the linear fit.

5 COMPUTING THE MASS–TO–LIGHT RATIOS

G98 give the virial masses M within R_{vir}, and Girardi et al. (1998a) use these masses to obtain those within $1.5\ h^{-1}$ Mpc by rescaling according to the galaxy distribution, which is assumed to follow the mass distribution. Here we obtain masses within 0.5 and $1.0\ h^{-1}$ Mpc by following a similar procedure.

By averaging the M/L_{B_j} values for C–clusters, we find no appreciable variation with increasing radius, as expected from the underlying assumption that mass follows galaxy distribution and from the scarce relevance of luminosity segregation (e.g. Biviano et al. 1992; Stein 1997). For each cluster we report in Table 3 (Col. 2) the minimum and maximum M/L_{B_j} values among those obtained by varying the radius, the data sample and the method to estimate luminosities. We also give the values of $M/L_{B_j,c}$ and $M/L_{B_j,f}$ within R_{vir} for clusters belonging to the C–sample (Cols. 3 and 4).

6 THE RELATIONS BETWEEN LUMINOSITY AND DYNAMICAL QUANTITIES

We draw our following results from the analysis of the 89 clusters of the C–sample, which is characterized by a homogeneous photometry and well defined completeness criteria. In particular, here we limit our analysis to mass and luminosities as computed within R_{vir} so that the correlations between cluster properties will be obtained at a fixed physical scale.

6.1 The L_{B_j}–σ_v relation

Considering the relation between luminosity and (line–of–sight) velocity dispersion, σ_v, has the advantage that the latter quantity is the directly observable one. In fact, the step from σ_v to virial mass estimate requires the additional assumption that mass distribution follows the galaxy distribution (cf. G98). We use the σ_v values, which can be considered representative of the total kinetic energy of galaxies, as given by G98 (see also Fadda et al. 1996).

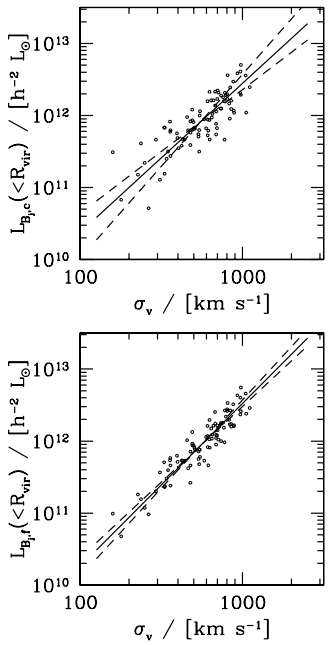

Fig. 4.— The relation between luminosity within R_{vir} and velocity dispersion. We consider both $L_{B_j,c}$ (top panel) and $L_{B_j,f}$ (bottom panel). Lines represent the linear fits: dashed lines give the direct and the inverse fits, while the solid line gives the bisecting line.

We fit a regression line in the logarithmic plane, $L_{B_j}/L_{B_j,\odot} = 10^a \sigma^b$ (see Figure 4). Using unweighted fits (Isobe et al. 1990), we calculate both the direct and the inverse, as well as the bisecting line. Since (random) errors on the variables are comparable ($\sim$ 20–30% for luminosities and 12% for velocity dispersions, cf. § 4.4 and G98) the bisecting line should provide the most appropriate regression relation. We obtain $a = 6.24 \pm 0.46$ and

TABLE 3

MASS–TO–LUMINOSITY RATIOS

Name	M/L_{B_j} (range) h $(M_\odot/L_\odot)$	$M/L_{B_j,c}$ (C–clusters) h $(M_\odot/L_\odot)$	$M/L_{B_j,f}$ (C–clusters) h $(M_\odot/L_\odot)$
A85	246-917	481	422
A119	143-313	181	143
A194	89-377	239	198
A229	173- 412	295	246
A256	147- 428	156	205
A295	71- 207	130	133
A420	249- 365	279	317
A426	280-458	-	-
A458	296-480	443	309
A496	288- 808	416	288
A514	500- 1131	687	500
A524	91- 230	91	170
A539	110-482	-	-
A576	588-736	-	-
A978	326- 619	424	326
A1060	162-327	216	162
A1069	121- 298	121	164
A1146	171- 247	191	171
A1314	40-43	-	-
A1631	149- 415	227	356
A1644	219- 285	251	251
A1656	121-225	-	-
A2040	128-181	-	-
A2151	287-351	-	-
A2197	257-385	-	-
A2256	560-876	-	-
A2353	170- 309	309	180
A2362	158- 398	398	269
A2401	145- 255	171	154
A2426	58- 202	70	202
A2500	204- 396	260	383
A2554	228-529	247	228
A2569	230- 510	315	230
A2593	173-283	-	-
A2644	62- 156	110	156
A2670	215-451	451	322
A2715	241- 421	274	408
A2717	154-446	466	308
A2721	184-454	280	200
A2734	413- 723	723	413
A2755	387- 500	412	426
A2798	90- 229	91	180
A2799	200- 312	312	221
A2800	184- 382	269	222
A2877	297- 639	449	297
A2911	95- 272	139	265
A3093	116- 197	175	153
A3094	316- 514	443	380
A3111	11- 53	17	53
A3122	647- 1340	1340	647
A3126	325-1080	711	325
A3128	261-369	369	325
A3142	345- 594	423	531
A3151	40- 131	48	125
A3158	360- 660	483	360
A3194	280- 552	432	280

TABLE 3

CONTINUED

Name	M/L_{B_j} (range) h ($M_\odot/L_\odot$)	$M/L_{B_j,c}$ (C–clusters) h ($M_\odot/L_\odot$)	$M/L_{B_j,f}$ (C–clusters) h ($M_\odot/L_\odot$)
A3223	301- 397	348	301
A3266	405- 547	473	405
A3334	282-650	568	320
A3354	71-156	71	107
A3360	461- 1007	1007	534
A3376	407- 766	669	407
A3381	45- 200	81	186
A3391	217- 366	222	221
A3395	355- 762	355	359
A3532	172- 251	172	188
A3556	165- 322	216	233
A3558	208-507	229	208
A3559	94- 134	134	123
A3571	179- 500	227	179
A3574	151-256	165	153
A3651	171- 200	184	200
A3667	277-551	288	293
A3693	100- 235	103	186
A3695	128- 187	187	145
A3705	232-439	254	232
A3733	329- 666	545	350
A3744	161- 203	191	161
A3809	223- 362	283	229
A3822	109- 127	116	124
A3825	218- 354	229	234
A3879	113- 216	140	132
A3880	294- 938	396	294
A3921	151- 198	168	151
A4008	187- 233	220	194
A4010	212- 325	308	253
A4053	298- 495	334	448
A4067	122- 168	131	122
S84	55- 90	55	74
S373	58- 242	242	84
S463	103- 126	126	123
S721	251- 596	274	254
S753	232-317	257	232
S805	143- 336	185	153
S987	126- 393	150	126
S1157	249-602	363	602
AWM1	127-148	-	-
AWM4	17-41	-	-
AWM7	917-1104	-	-
DC0003-50	142- 286	178	142
Eridanus	50- 776	776	417
MKW1	74- 127	109	91
MKW4	319-367	-	-
Ursa Major	164-252	-	-
Virgo	242-459	-	-

$b = 2.07 \pm 0.16$ for $L_{B_j,c}$ (with $b = 1.72$ and 2.56 for the direct and inverse fits) and $a = 5.73 \pm 0.27$ and $b = 2.26 \pm 0.10$ for $L_{B_j,f}$ (with $b = 2.10$ and 2.45 for the direct and inverse fits). The scatter is $\sim 25\%$ for $L_{B_j,c}$ and $\sim 15\%$ for $L_{B_j,f}$.

Alternatively, we also apply a weighted regression line (e.g. Press et al. 1992), by varying the errors on $L_{B_j,f}$ in the range of 20–30% and considering both a 12% error in σ_v and the nominal σ_v errors given by G98. We find that

b varies in the ranges 2.0–2.5 and 2.2–2.4 for $L_{B_j,c}$ and $L_{B_j,f}$, respectively. Moreover, the small scatter in the $L_{B_j,f}$–σ_v relation can be accounted for by the assumed errors. On the contrary, the large scatter of $L_{B_j,c}$–σ_v can not be completely accounted for by errors in $L_{B_j,c}$ and σ_v.

The better defined correlation with σ_v suggests that the $L_{B_j,f}$ values are less affected by random errors than $L_{B_j,c}$. This is consistent with the fact that $L_{B_j,f}$ is computed by using local field subtractions, while mean field corrections are applied for the $L_{B_j,c}$ computation.

6.2 The M/L_{B_j} ratios and the M – L_{B_j} relation

We find $M/L_{B_j,c} = 251^{+28}_{-29}$ and $M/L_{B_j,f} = 229^{+22}_{-29}$ for the median values of the mass-to-light ratios, with errors corresponding to 90% c.l. intervals.

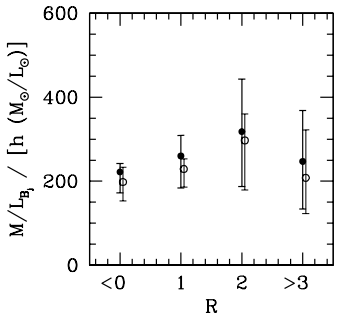

Fig. 5.— The behaviour of mass–to–light ratio vs. cluster richness. Points are median values with 90% c.l. error bars. Solid and open points come from $L_{B_j,c}$ and $L_{B_j,f}$ estimates, respectively.

In order to explore the behavior of M/L_{B_j} with respect to cluster properties, we look for possible correlations with cluster morphology, i.e Bautz–Morgan type (86 clusters, types taken from Abell, Corwin, & Olowin 1989), Rood–Sastry type (40 clusters, types taken from Struble & Rood 1987 and from Struble & Ftaclas 1994), and with cluster richness class R. We find only a weak significant correlation with R (i.e. $\sim 95\%$ c.l.). Figure 5 shows the median M/L_{B_j} vs. R where M/L_{B_j} increases with R and then flattens for the richest $R \geq 3$ clusters.

In order to better examine a possible increasing of M/L_{B_j} from poor to rich structures, we avoid analyzing the behavior of M/L_{B_j} vs. M or L_{B_j} because M/L_{B_j} is defined as a function of M and L_{B_j}, and therefore we were plotting correlated quantities (see, e.g., Mezzetti, Giuricin, & Mardirossian 1982). Instead, we directly examine the M–L_{B_j} relation by fitting a regression line in the logarithmic plane,

$$\frac{M}{M_\odot} = 10^c \cdot \left(\frac{L_{B_j}}{L_{B_j,\odot}}\right)^d . \qquad (3)$$

As for the $L_{B_j,f}$ luminosity, we obtain $c = -0.34 \pm 0.72$ and $d = 1.22 \pm 0.06$ for the unweighted bisecting fit, with a scatter of $\sim 30\%$ (see Figure 6). As for the weighted regression fit, by varying the errors on $L_{B_j,f}$ in the range 20–30% and considering a global error on M by 40%, or alternatively the nominal mass errors given by G98, we obtain that d varies in the range 1.17–1.23, again significantly larger than unity.

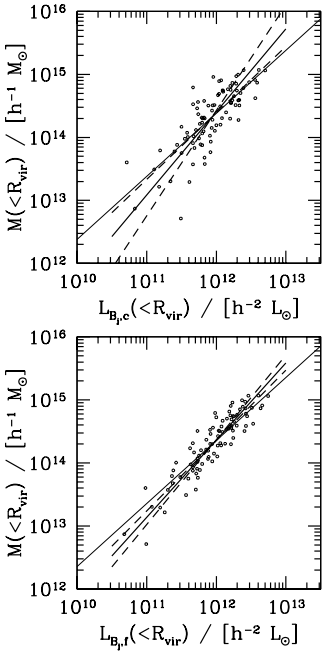

Fig. 6.— The relation between mass and luminosity within R_{vir}. We consider both $L_{B_j,c}$ (top panel) and $L_{B_j,f}$ (bottom panel). Heavy lines represent the linear fits: dashed lines give the direct and the inverse fits, while the solid line gives the bisecting line. The faint line is the $M \propto L_{B_j}$ fitted relation.

As for the $L_{B_j,c}$ luminosity, the fitted bisecting line gives $c = -1.41 \pm 1.30$ and $d = 1.32 \pm 0.11$ with a scatter of $\sim 45\%$. The weighted analysis gives $d = 1.06$–1.33 and, again, the large scatter in the M–$L_{B_j,c}$ relation is not completely justified by the assumed errors.

6.3 The Robustness of the M–L_{B_j} Relation

We have discussed in § 4 the possible systematics affecting the estimates of cluster luminosities. Although we have shown that such systematics should not introduce strong biases in L_{B_j}, it is anyway worth investigating their effects on the M–L_{B_j} relation, being the tendency of cluster mass to increase faster than luminosity a small (although significant) effect [cf. eq.(3)].

As for the background corrections, we first note that, although the methods for their estimate for $L_{B_{j,c}}$ and $L_{B_{j,f}}$ are completely independent, the two resulting mass-luminosity relations (M–$L_{B_j,c}$ and M–$L_{B_j,f}$) well agree both in slope and in normalization.

An increase in the amount of mean field counts for the $L_{B_j,c}$ correction has the effect of reducing more the luminosities of poorer clusters. For instance, the use of the

20% larger background correction by Colless (1989) decreses the exponent d in eq.(3) only from 1.32 to 1.28. In order to make it consistent with unity at 2-sigma c.l., one has to assume that the L97 counts underestimate the true background by about 40%. This seems rather unlikely, in view of the similarity between the results by L97 and Maddox et al. (1990b), which are the two analysis based on the largest analyzed area.

A possible way to change the slope of the M–$L_{B_j,f}$ relation would be to have a dependence on the cluster mass for the depth of the redshift samples, from which the f_L fractions are estimated. However, when using the homogeneous subsample of 51 clusters for which the f_L values are obtained from ENACS data (cf. § 4.1) we find the same M–$L_{B_j,f}$ relation, with slope $d = 1.21$.

A larger increase of luminosities for richer clusters can also be the consequence of more negative α values in the Schechter LF which is used to extrapolate the cluster luminosity to faint galaxy magnitudes (cf. § 4.2). For $\alpha = -1.5$ we obtain $d = 1.20$ and 1.28 for $L_{B_j,f}$ and $L_{B_j,c}$, respectively, while $\alpha = -1.9$ is required to reconcile d with unity within 2-sigma c.l. However, current observations indicates that the LF can be so steep only at very faint magnitues. When using the LF model discussed in § 4.2, i.e. a Schechter function coupled with a power–law, we still find $d > 1$ at 2.5–3 sigma c.l. even considering the rather extreme case $\alpha = -1.5$ and $\beta = -2$ for the exponents of the Schechter and power–law parts of the LF, respectively.

As for the effect of possible systematic variations of the LF both from cluster to cluster and within each cluster, several works considered the dependence of the galaxy LF on cluster radius and found no significant changes (e.g. Colless 1989; Metcalfe et al. 1994; Valotto et al. 1997; Rauzy et al. 1998), thus in agreement with evidences that luminosity segregation concerns only very luminous galaxies (e.g. Biviano et al. 1992; Stein 1997). A recent analysis of seven clusters at $z \sim 0.15$ (Driver et al. 1998) shows that the fraction of dwarf–to–giant galaxies depends on the physical region analyzed and increases significantly from the inner to the outer cluster region. However, we expect this not to represent a serious concern for our analysis, since our results are based on luminosities all computed within the physical radius R_{vir}.

A relevant point in the determination of the slope of the M–L_{B_j} relation concerns the universality of the LF. Indeed, a flatter LF for less massive clusters could in principle reconcile the observed relation with $M \propto L_{B_j}$. L97 found no clear evidence for LF variations with the Bautz–Morgan class, BM, or richness (see also Lugger 1986; Colless 1989; Trentham 1998; and recently Rauzy et al. 1998 for ENACS clusters). However, there is a tendency to find that clusters with a dominant cD galaxy and/or $BM = 1$, high richness and regular X–ray emission have flat LF (e.g. Dressler 1978b; López et al. 1997; see however Valotto et al. 1997). From a recent analysis of seven clusters down to faint magnitudes ($M_R = -16.5$), Driver et al. (1998) found that the ratio of dwarf–to–giant galaxies decreases (from 3.1 to 0.8) with the mean local projected galaxy density (cf. also Garilli, Maccagni, & Andreon 1998). This turns into a flatter LF in more dense environments, with α varying from –0.9 to –1.4. In general, the global cluster parameter which correlates with the LF slope seems to be the morphological type, rather than the cluster richness (e.g., Driver et al. 1998). Indeed, there is a well known correspondence among different cluster classifications, where regular clusters are usually of early Bautz-Morgan or Rood-Sastry types, with high central galaxy density and elliptical–rich systems (see Bahcall 1977 for a review).

A clear evidence for a correlation between cluster regularity (or density) and mass has been not found to date, although indications in this direction have been provided, for instance, by the correlation between regularity and X–ray luminosity (e.g. Forman & Jones 1982 for a review). Therefore, if any, the effect of a correlation between cluster mass and LF slope would go in the direction of increasing the slope d of the M–L_{B_j} relation.

Finally, we consider the possibility that cluster substructures can contribute to increase the scatter or to change the slope of the M–L_{B_j} relation. We extract only those 54 clusters for which the significance for the presence of substructures is $< 90\%$, according to a Dressler–Schectman test (Dressler & Schectman 1988) applied to the reference redshift samples of G98. We find consistent results for the slope of the M–L_{B_j} relation and no reduction of its scatter.

7 DISCUSSION

7.1 The L–σ_v Relation

Our result that $L_{B_j} \propto \sigma_v^{2.1\text{–}2.3}$, for L_{B_j} estimated within the virialization radius R_{vir}, can be compared to previous determinations, at least for those cases where luminosities are measured within some physical radius. Schaeffer et al. (1993), who used the total cluster luminosities by West, Oemler, & Dekel (1989), found $L_V \propto \sigma_v^{1.87\pm0.44}$. Adami et al. (1998a), who estimated luminosities within a square of 10 core–radii of diameter, found $L_{B_j} \propto \sigma_v^{1.56}$ but with a large scatter. Steeper relations are found for a variety of smaller systems, e.g. $L_V \propto \sigma_v^{2.3}$ for globular clusters (Paturel & Garnier 1992), $L_B \propto \sigma_v^{2.5}$ for dwarf ellipticals (Held et al. 1992), and $L \propto \sigma_v^{3.5\text{–}4}$ for ellipticals (e.g. Faber & Jackson 1976; Dressler et al. 1987).

Some authors, by analyzing clusters in analogy with elliptical galaxies, found a relation betwen luminosity, cluster size R and velocity dispersion of the type $L \propto R^A \sigma_v^B$. Typical values for the parameters defining this cluster fundamental plane range in the intervals $A = 0.9\text{–}1.4$ and $B = 0.9\text{–}1.3$ (Schaeffer et al. 1993; Adami et al. 1998a). Since for a virialized structure we expect its scale to be proportional to the internal velocity dispersion, the above scaling relations would traslate into $L \propto \sigma_v^{1.8\text{–}2.7}$ thus in agreement with our findings. A detailed fundamental plane analysis for our cluster sample will be deserved to a

forthcoming paper.

7.2 The M–L Relation

One of the main results of our analysis is that mass has a slight, but significant, tendency to increase faster than the luminosity. In particular, we find that $M \propto L_{B_j}^{1.2-1.3}$, which translates into a M/L_{B_j} variation of a factor of 2–3 from poor to rich clusters. Again, this result can be related to those inferred from the analysis of the cluster fundamental plane. In fact, assuming the virialization state and internal structure of all clusters to be identical, Schaeffer et al. (1993) found that $M/L_V \propto L_V^{0.3}$ and Adami et al. (1998a) showed that $M/L_{B_j} \propto \sigma_v$ (i.e. $\propto M^{1/3}$ for the mass contained within the virialized region, cf. G98). In general there is no evidence of correlation between M/L and cluster properties (e.g. Dressler 1978b; Carlberg et al. 1996; Fritsh & Buchert 1999; see, however, Adami et al. 1998b, who found a correlation with σ_v). Due to the small size of the effect we detected, it is clear that it can be seen only in a rather large cluster sample spanning a large dynamical range.

In § 6.3 we verify the robustness of the M–L_{B_j} against possible systematics. Here we analyze the possibily that the fitted slope might be completely driven by the kind of photometry of our sample. Since late–type galaxies are bluer than early–type galaxies, a possible over-abundance of late–type galaxies in poor clusters could flatten the observed relation between masses and luminosities coming from V or R photometry.

It is well known that the late–type galaxy fraction decreases with the local density (Dressler et al. 1980) and increases with the distance from the cluster center (Whitmore, Gilmore, & Jones 1993). Since, as already discussed in § 6.3, there is no well established correlation between cluster density and mass, it is difficult to establish a morphology–richness correlation. In fact, Whitmore et al. (1993) found that the behaviour of morphology vs. radius is independent of σ_v. However, if we assume that this relation does indeed exist and poor clusters are really spiral–richer, we can attempt a simple calculation of the effect of working with R photometry instead with B one (since we use B_j instead of B the true effect would be also smaller). Since $B_\odot = 5.48$ and $R_\odot = 4.31$ (Allen 1973) and being $(B-R) \sim 1.5$ for early type galaxies and $(B-R) \sim 1$ for spirals of de Vaucouleurs type 5 (Buta et al. 1994 and Buta & Williams 1995), we find that $L_R^e = 1.3 L_B^e$ for luminosity of early–type galaxies and $L_R^l = 0.8 L_B^l$ for luminosity of late type galaxies. Then, when assuming that typical galaxy luminosities in clusters are roughly comparable for early and late type galaxies (e.g. Sandage, Binggeli, & Tammann 1985; Andreon 1998) and that the ratio between early-to-late type galaxies goes from 3.5 to 1 for spiral–poor and spiral–rich clusters, respectively (e.g. Oemler 1974), we obtain $L_R \sim 1.20 L_B$ and $L_R \sim 1.05 L_B$ for spiral–poor and spiral–rich clusters, respectively. Even assuming that these different conversions must be applied to clusters whose mass is larger and smaller that the median value, respectively, we obtain $M \propto L_R^d$ with $d > 1$ at 2.5–sigma c.l.

Therefore, although we suggest that a conclusive result could be found only by directly analyzing other samples in different magnitude bands, we find at present no evidence that our mass–dependent M/L relation can be explained by a higher spiral fraction in poorer clusters.

7.3 The M/L ratios

Median values of M/L_{B_j} are found to range in the interval 230–250 $h\, M_\odot/L_\odot$, thus in good agreement with recent estimates (e.g. David et al. 1995) and definitely lower than older estimates (cf. Faber & Gallagher 1979). Our M/L_{B_j} ratios are smaller than those by Adami et al. (1998b). Since their luminosities are comparable to ours, this difference is due to the smaller masses fund by G98. Our M/L_{B_j} ratio agrees with that by Carlberg et al. (1996, $M/L_R \sim 300$), whose optical virial masses are have been shown to be consistent with X–ray masses (Lewis et al. 1999; note that the change of luminosity due to evolutionary effects roughly cancels the change of luminosity betweeen R and B bands).

The assumption that M/L within clusters is typical of the Universe as a whole leads to an estimate of the matter density parameter Ω_m (hereafter $(\Omega_m)_{M/L}$), e.g. Bahcall et al. 1995; Carlberg et al. 1996), which has the advantage of being independent of the value of H_0 and of the presence of a cosmological constant. Estimates of the B–band luminosity density gives $\rho_L \simeq 2 \times 10^8 h\, L_\odot$ Mpc^{-3} (Efstathiou, Ellis & Peterson 1988; Zucca et al. 1997; Loveday, Tresse & Maddox 1999), which corresponds to the M/L_B closure value of $\simeq 1350\ h\, M_\odot/L_\odot$. Although we take this value in the following as the reference one, we remind that its determination is quite sensitive to uncertainties in the local galaxy luminosity function (cf. Marinoni et al. 1999). With the above value for the closure M/L_B, we obtain $(\Omega_m)_{M/L} \simeq 0.2$, in agreement with recent determinations of Ω_m based, for instance, the M/L ratio of distant CNOC clusters (Carlberg et al. 1996), on the gas fraction within clusters (e.g. Evrard 1997) and on combining high–z SNIa data with preliminary measurements of small scale CMB anisotropies (e.g. Tegmark 1999).

As already noted by Rees (1985), an increase of M/L with the scale of the collapsed structure within which it is estimated can in principle reconcile the observed cluster M/L values with $\Omega_m = 1$. This could be possible in the framework of biased galaxy formation (e.g. Kaiser 1984; Bardeen et al 1986) and, indeed, various physical mechanisms could produce large–scale variations in the conversion efficiency from baryons to luminous galaxies (e.g. Rees 1985; Blumenthal et al. 1984; Dekel & Rees 1987) leading to $(\Omega_m)_{M/L} \leq \Omega_m$. Although the difference between efficiencies of gas conversion into stars for field and clusters is not yet precisely known, reconcilying such low M/L values with a critical density Universe would require a difference in such efficiencies by at least a factor three. Furthermore, the mild increase of M/L with cluster luminosity that we find is more consistent with a low–density and low–bias model, rather than with a high–bias critical–

density model.

8 SUMMARY AND CONCLUSIONS

We analyze a sample of 105 galaxy clusters for which Girardi et al. (1998b, G98) computed virial masses, all having available galaxy magnitudes with some degree of completeness. In particular, our main result on the cluster mass–to–light ratio are drawn from a subsample of 89 clusters with B_j band galaxy magnitudes taken from the survey of COSMOS/UKST Southern Sky Object Catalogue (Yentis et al. 1992). Photometry for other clusters is provided at different magnitude bands.

After suitable magnitude corrections and uniform conversions to the B_j band, we compute cluster luminosities within several clustercentric radii, $0.5, 1.0, 1.5\ h^{-1}$ Mpc, and within the virialization radius R_{vir}. To this purpose, we use the results by Lumsden et al. (1997, L97) on the luminosity functions and galaxy counts for the EDSGC, which is the well-calibrated part of the COSMOS catalogue.

We analyze the effect of several uncertainties connected with original photometric data, our corrections/conversions of galaxy magnitudes, fore/background subtraction, and extrapolation below the completeness limit of the photometry. In particular, we find an overall agreement between luminosities computed by applying two independent methods of fore/background correction, one based on mean galaxy counts, $L_{B_j,c}$, and one taking into accounts the local cluster field, $L_{B_j,f}$. We find that both random and possible systematic errors on luminosities are about $20-30\%$. We compute and list M/L ratios for the 105 clusters.

In order to examine the relations between cluster luminosities and dynamical quantities we consider only the homogeneus sample (C–sample) taken from the COSMOS catalogue. In this way, we avoid possible errors connected to magnitude band conversions and have the advantage of dealing with a well defined magnitude completeness. Using the COSMOS magnitudes is also consistent with our choice to use the L97 results on luminosity function and galaxy counts in the luminosity calculations. Cluster luminosities are computed within the virialization radius for all clusters.

Our main results can be summarized as follows.

(a) We find a well–defined correlation between cluster luminosity and galaxy velocity dispersion, $L \propto \sigma_v^{2.1–2.3}$, with a scatter of $\sim 15\%$ and $\sim 25\%$ for $L_{B_j,f}$ and $L_{B_j,c}$, respectively. As expected the luminosities $L_{B_j,f}$ based on a local field correction shows smaller random errors than $L_{B_j,c}$, which is based on a mean field correction.

(b) Different methods to estimate luminosities provide median mass–to–light ratios with typical values $M/L_{B_j} \sim$ 230–250 $h\, M_\odot/L_\odot$. We do not find any correlation of M/L_{B_j} with cluster morphologies, i.e. Rood–Sastry and Bautz–Morgan types, and only a weak significant correlation with cluster richness.

(c) We find a good correlation between cluster luminosity and mass. In particular, mass has a slight, but significant, tendency to increase faster than the luminosity does, $M \propto L_{B_j}^{1.2–1.3}$. The scatter is $\sim 30\%$ and $\sim 45\%$ for $L_{B_j,f}$ and $L_{B_j,c}$, respectively. We verify the robustness of this relation and show that the $M \propto L_{B_j}$ relation is very difficult to be reconciled with available data.

Finally, by using a simple approach, we verify that the tendency of mass to increase faster than the luminosity cannot be explained by a higher spiral fraction in poorer clusters. Therefore, we suggest that a similar result should also be found when analyzing a cluster sample with R band galaxy magnitudes. However, a more conclusive result on this point should wait for a direct analysis of R band magnitude samples.

We thank F. Durret and N. Metcalfe for having given us the electronic version of their catalogs. We are particularly in debt with Sandro Bardelli for having giving us his compilation of A3558 cluster and for enlighting suggestions, too. We also thank Andrea Biviano, Peter Katgert, Massimo Persic, Massimo Ramella, Paolo Salucci, and Dario Trevese, for useful discussions. Special thanks to Alessandro Cristofoli for his help in initial phase of this project. We thank an anonymous referee for useful suggestions. S.B. wishes to acknowledge Osservatorio Astronomico and ICTP in Trieste for the hospitality during the preparation of this work. This research has made large use of the COSMOS/UKST Southern Sky Catalogue supplied by the Anglo–Australian Observatory. This work has been partially supported by the Italian Ministry of University, Scientific Technological Research (MURST), and by the Italian Space Agency (ASI).

REFERENCES

Abell, G. O., Corwin, H. G. Jr., & Olowin, R. P. 1989, ApJS, 70, 1
Adami, C., Mazure, A., Biviano, A., Katgert, P., & Rhee, G. 1998a, A&A, 331,493
Adami, C., Mazure, A., Katgert, P., & Biviano, A. 1998b, A&A, 336, 63
Allen, C. W. 1973, Astrophysical Quantities, London: University of London, Athlane Press
Allen, S. W. 1997, MNRAS, 296, 392
Andreon, S. 1998, A&A, 336, 98
Bahcall, N. A. 1977, ARA&A, 15, 505
Bahcall, N. A., Lubin, L. M., & Dorman, V. 1995, ApJ, 447, L81
Bardeen, J. M., Bond, J. R., Kaiser, N., & Szalay, A. S 1986, ApJ, 304, 15
Bardelli, S., Zucca, E., Zamorani, G., Vettolani, G., & Scaramella, R. 1998, MNRAS, 296, 599
Barmby, P., & Huchra, J. P. 1998, AJ, 115, 6
Beers, T. C., Geller, M. J., Huchra, J. P., Latham, D. W., & Davis, R.J. 1984, ApJ, 283, 33
Binggeli, B., Sandage, A., & Tammann, G. A. 1985, AJ, 90, 1681
Biviano, A., Durret, F., Gerbal, D., Le Févre, O., Lobo, C., Mazure, A., & Slezak, E. 1995, A&A, 297, 610
Biviano, A., Girardi, M., Giuricin, G., Mardirossian, F., & Mezzetti, M. 1992, ApJ, 396, 35

Blair, M., & Gilmore, G. 1982, PASP, 94, 742
Blumenthal, G. R., Faber, S. M., Primack, J. R., & Rees, M. J. 1984, Nature, 311, 517
Buta, R., Mitra, S., de Vaucouleurs, G., & Corwin, H. G. Jr. 1994, AJ, 107, 118
Buta, R., & Williams, K. L. 1995, AJ, 109, 543
Carlberg, R. G., Yee, H. K. C., Ellingson, E., Abraham, R., Gravel, P., Morris, S., & Pritchet, C. J., et al. 1996, ApJ, 462, 32
Chapman, G. N. F., Geller, M. J., & Huchra, J. P. 1988, AJ, 95, 999
Colless, M. 1989, MNRAS, 237, 799
David, L. P., Jones, C., & Forman, W. 1995, ApJ, 445, 578
de Vaucouleurs, G., de Vaucouleurs, A., Corwin, H.G., Buta, R.J., Paturel, G. & Fouqué, P. 1991, "3^{rd} Reference Catalogue of Bright Galaxies", $9th$ version.
Dekel, A., & Rees, M. 1987, Nature, 326, 455
De Propris, R., & Pritchet, C. J. 1998, AJ, 116, 1118
Dressler, A. 1978a, ApJ, 223, 765
Dressler, A. 1978b, ApJ, 226, 55
Dressler, A., Lynden-Bell D., Burstein, D., Davis, R., Faber, S., Wagner, M., & Terlevich, R. 1987, ApJ, 313, 42
Dressler, A., & Shectman, S. A. 1988, AJ, 95, 985
Drinkwater, M. J., Barnes, D. G., & Ellison, S. 1995, PASA, 12, 248
Driver, S. P., Couch, W. J., & Phillipps, S. 1998, MNRAS, 301, 369
Ebeling, H., Edge, A. C., Fabian, A. C., Allen, S. W., Crawford, C. S., & Böhringer, H. 1997, ApJ, 479, L101
Efstathiou, G., Ellis, R.S., & Peterson, B.A., 1988, MNRAS, 232, 431
Evrard, A. E. 1997, MNRAS, 292, 289
Eyles, C. J., Watt, M. P., Bertram, D., Church, M. J., Ponman, T. J., Skinner, G. K., & Willmore, A. P. 1991, ApJ, 376, 23
Faber, S. M. , & Gallagher, J. S. 1979, ARA&A, 17, 135
Faber, S. M. , & Jackson, R. 1976, ApJ, 204, 668
Fabricant, D. G., Kent, S. M., & Kurtz, M. J. 1989, ApJ, 336, 77
Fabricant, D., Kurtz, M., Geller, M., Zabludoff, A., Mack, P., & Wegner, G. 1993, AJ, 105, 788
Fadda, D., Girardi, M., Giuricin, G., Mardirossian, F., & Mezzetti, M. 1996, ApJ, 473 670
Flin, P., Trevese, D., Cirimele, G., & Hickson, P. 1995, A&AS, 110, 313
Forman, W., & Jones, C. 1982, ARA&A, 20, 547
Fritsch, C., & Buchert, T. 1999, A&A, 344, 749
Garilli, B., Maccagni, D., & Andreon, S. 1998, accepted for publication in A&A, 342, 408
Geller, M. J., et al. 1997, AJ, 114, 2205
Girardi, M., Fadda, D., Escalera, E., Giuricin, G., Mardirossian, F., & Mezzetti, M. 1997, ApJ, 490, 56
Girardi, M., Borgani, S., Giuricin, G., Mardirossian, F., & Mezzetti, M. 1998a, ApJ, 506, 45
Girardi, M., Giuricin, G., Mardirossian, F., Mezzetti, M., & Boschin W. 1998b, ApJ, 505, 74 (G98)
Godwin, J. G., Metcalfe, N., & Peach, J. V. 1983, MNRAS, 202, 113
Gregory, S. A., & Thompson, L. A. 1984, ApJ, 286, 422
Held, E. V., de Zeeuw, T., Mould, J., & Picard, A. 1992, AJ, 103, 851
Heydon-Dumbleton, N. H., Collins, C. A., & MacGillivray, H. T. 1988, in Large-Scale Structures of the Universe – Observational and analytical methods, Proceedings of the Workshop, Bad Honnef, Federal Republic of Germany, Berlin and New York, Springer-Verlag, 1988, p. 71
Heydon-Dumbleton, N. H., Collins, C. A., & MacGillivray, H. T. 1989, MNRAS, 238, 379
Kaiser, N. 1984, ApJ, 284, L9
Katgert, P., Mazure, A., den Hartog, R., Adami, C., Biviano, A., & Perea, J. 1998, A&AS, 129, 399
Kent, S. M., & Gunn, J. E. W. 1983, AJ, 87, 945
Kent, S. M., & Sargent, W. L. W. 1983, AJ, 88, 1094
Kirshner, R. P., Oemler, A., & Schechter, P. L. 1978, AJ, 83, 1549
Kron, R. G. 1978, PhD thesis, Univ. California, Berkeley
Isobe, T., Feigelson, E. D., Akritas, M. G., & Babu, G. J. 1990, ApJ, 364, 104
Jørgensen, I. 1994, PASP, 106, 967
Lewis, A. D., Ellingson, E., Morris, S. L., & Carlberg, R. G. 1999, ApJ, 517, 587
Lopez-Cruz, O., Yee, H. K. C., Brown, J. P., Jones, C., & Forman, W. 1997, ApJ, 475, L97
Loveday, J., Tresse, L., & Maddox S. 1999, MNRAS, in press, preprint astro-ph/9905385
Lugger, P. M. 1986, ApJ, 303, 535
Lugger, P. M. 1989, ApJ, 343, 572
Lumsden, S. L., Collins, C. A., Nichol, R. C., Eke, V. R., & Guzzo, L. 1997, MNRAS, 290, 119 (L97)
Maddox, S. J., Efstathiou, G. P., & Sutherland, W. J. 1990a, MNRAS, 246, 433
Maddox, S. J., Sutherland, W. J., Efstathiou, G. P., Loveday, J., Peterson, B. A. 1990b, MNRAS, 247, 1P
Malumuth, E. M., & Kriss, G. A. 1986, ApJ, 308, 10
Marinoni, C., Monaco, P., Giuricin, G., & Costantini, B. 1999, ApJ, in press, preprint astro-ph/9903394
Metcalfe, N., Fong, R., & Shanks, T. 1995, MNRAS, 274, 769
Metcalfe, N., Godwin, J. G. & Peach, J. V. 1994, MNRAS, 267, 431
Mezzetti, M., Giuricin, G., & Mardirossian, F. 1982, ApJ, 259, 30
Mohr, J. J., Geller, M. J., Fabricant, D. G., Wegner, G., Thorstensen, J., Richstone, D. O. 1996, ApJ, 470, 724
Narayan, R., & Bartelmann, M. 1996, in Formation of Structure in the Universe, eds. A. Dekel and J.P. Ostriker (Cambridge University Press), preprint astro-ph/9606001
Oemler, A. Jr. 1974, ApJ, 194, 1
Ostriker, E. C., Huchra, J. P., Geller, M. J. & Kurtz, M. J. 1988, AJ, 96, 1775
Paturel, G., & Garnier, R. 1992, A&A, 254, 93
Press, W. H., Teukolsky, S. A., Vetterling, W. T., & Flannery, B. P. 1992, Numerical Recipes (2d ed.; Cambridge: Cambridge Univ. Press)
Rauzy, S., Adami, C., & Mazure, A. 1998, A&A, 337, 31
Rees, M. J. 1985, MNRAS, 213, P75
Richter, O. G. 1989, A&AS, 77, 237
Roberts, M. S. & Haynes, M. P. 1994, ARA&A, 32, 115
Rubin, V. C. 1993, Proc. Natl. Acad. USA, 90, 4814
Sandage, A. 1973, ApJ, 183, 711
Sandage, A., Binggeli, B., & Tammann, A. 1985, AJ, 90, 1759
Schaeffer, R., Maurogordato, S., Cappi, A., & Bernardeau, F. 1993, MNRAS, 263, L21
Shanks, T., Stevenson, P. R. F., & Fong, R. 1984, MNRAS, 206, 767
Sharples, R. M., Ellis, R. S., & Gray, P. M. 1988, MNRAS, 231, 479
Schechter, P. 1976, ApJ, 203, 297
Slezak, E., Durret, F., Guibert, J., Lobo, C. 1998, A&AS, 128, 67
Sodré, L., Capelato, H. V., Steiner, J. E., Proust, D., & Mazure, A. 1992, MNRAS, 259, 233
Stein, P. 1997, A&A, 317, 670
Struble, M. F., & Ftaclas, C. 1994, AJ, 108, 1
Struble, M. F., & Rood, H. J. 1987, ApJS, 63, 555
Tegmark, M. 1999, ApJ, 514, L69
Trentham, N. 1998, MNRAS, 293, 71
Trevese, D., Cirimele, G., & Appodia, B. 1996, A&A, 315, 365
Trevese, D., Cirimele, G., Cenci, A., Appodia, B., Flin, P., Hickson, P. 1997, A&AS, 125, 459
Tully, R. B., Verheijen, M. A. W., Pierce, M. J., Huang, J., & Wainscoat, R. J. 1996, 112, 2471
Valotto, C. A., Nicotra, M. A., Muriel, H., & Lambas, D. G. 1997, ApJ, 479, 90
West, M. J., Oemler, A. Jr., & Dekel, A. 1989, ApJ, 346, 545
Whitmore, B. C., Gilmore, D., M., & Jones, C. 1993, ApJ, 407, 489
Willmer C. N. A., Focardi P., Chan R., Pellegrini P. S., & da Costa, L. N. 1991, AJ, 101, 57
Wu, X. P., & Fang, L. Z. 1997, ApJ, 483, 62
Yentis, D., Cruddace, R., Gursky, H., Stuart, B., Wallin, J., MacGillivray, H., & Collins, C. 1992, in Digitised Optical Sky Survey, p. 67, eds. MacGillivray, H. T., & Thomson, E. B., Kluwer Academic Publisher, Dordrecht, Boston, MA.
Zabludoff, A., & Zaritsky, D. 1995, ApJ, 447, L21
Zucca, E., et al., 1997, A&A, 326, 477

Zwicky, F. 1933, Helv. Phys. Acta, 6, 10